

Malignancy-associated changes in breast tissue detected by image cytometry

Ellen C.M. Mommers^a, Neal Poulin^b,
Chris J.L.M. Meijer^a, Jan P.A. Baak^c
and Paul J. van Diest^{a,*}

^a *Department of Pathology, Free University Hospital, Amsterdam, The Netherlands*

^b *Cancer Imaging Department, Medical Physics Division, British Columbia Cancer Agency, Vancouver, British Columbia, Canada*

^c *Medical Center Alkmaar, Alkmaar, The Netherlands*

Received 24 January 2000

Accepted 27 July 2000

In several tissues, nuclear differences have been described in normal-appearing cells from patients with invasive carcinomas compared to cases without invasive carcinoma, a phenomenon known as malignancy-associated changes (MACs). The aim of this study was to determine the presence of malignancy-associated changes in breast tissue.

Image cytometry was performed on Feulgen stained tissue sections of patients with usual ductal hyperplasia with ($n = 30$) or without ($n = 41$) adjacent invasive breast carcinoma. Nuclear features of normal-appearing cells as well as of usual ductal hyperplastic cells were separately compared between the two groups.

Many features of normal-appearing epithelial cells were significantly different between cases with and without invasive cancer. Significant differences were also found by measuring ductal hyperplastic nuclei instead of normal-appearing nuclei. Cases with or without cancer could be distinguished with a classification accuracy of 80% by discriminant analysis using 2 nuclear features derived from ductal hyperplastic cells.

In conclusion, image cytometry on breast tissue sections shows that malignancy-associated changes can be found in normal as well as in usual ductal hyperplastic breast cells. This could be clinically relevant for the detection of occult breast cancer, for the prediction of risk in these lesions, and to monitor the effect of chemopreventive agents.

Keywords: Image cytometry, chromatin, texture, breast, malignancy-associated changes, hyperplasia

1. Introduction

Image cytometry has been performed on many tissues and may be used for diagnostic purposes and prediction of prognosis of patients with (pre)malignant lesions [2,3,6,8,11,13,15]. Besides measuring nuclear features of (pre)malignant tumor cells, information can also be derived from nuclear measurements on normal-appearing cells. Several studies found subtle differences in nuclear features in normal-appearing cells in patients with invasive carcinomas compared to cases without invasive carcinoma, a phenomenon known as malignancy-associated changes (MACs) [2, 4,10,12,14,16,17,19,20,22,23,26,27]. Over 85% of the sections of patients with or without lung cancer could correctly be classified as having cancer or not by image cytometric measurements on the normal-appearing lung cells [19]. Cases with prostatic adenocarcinoma could be separated from cases with benign prostatic hyperplasia with a sensitivity and specificity of over 90% using image cytometry on histologically normal-appearing cells [20]. Also in cervical smears and tissue, normal-appearing cells of cases with invasive cancer have significantly different nuclear features compared to cases without invasive cancer [2,4,12,14,16, 17,22,26]. Furthermore, it was found that the intensity of MACs were directly related to the severity of the adjacent cervical lesion [12]. These results imply that image cytometry on normal-appearing cells could be used to detect the presence of invasive carcinoma (at distant) and that it may be used in screening and chemoprevention studies.

Malignancy-associated changes detected with image cytometry have also been described in breast tissue, although the statistical power to distinguish between cases with or without cancer was low [27]. Other indications that MACs exist in breast tissue were found in genetic studies, in which loss of heterozygosity and

*Corresponding author: Paul J. van Diest, MD, PhD, Department of Pathology, Free University Hospital, P.O. Box 7057, 1007 MB Amsterdam, The Netherlands. Tel.: +31 20 444 4080; Fax: +31 20 444 2964; E-mail: pj.vandiest@azvu.nl.

microsatellite instability was seen in morphologically normal lobules adjacent to breast cancers [7,18]. However, not many studies have been performed on breast tissue to detect MACs. In the present study, we performed image cytometry on normal-appearing breast cells from cases with or without invasive cancer in order to detect nuclear features that could predict the presence of invasive cancer. Furthermore, we compared usual ductal hyperplastic lesions, some of which are considered to be early precursors of breast cancer, of cases with and without cancer to detect possible image cytometric differences in these cells.

2. Material and methods

2.1. Material

Seventy-one usual ductal hyperplasias of the breast (25 mild, 26 moderate, 20 florid) were collected from the archives of the Department of Pathology of the Free University Hospital in Amsterdam, the Netherlands. Of these cases, 30 (42%) had adjacent invasive breast cancer. The distribution of mild, moderate, and florid ductal hyperplasias was comparable for cases with and without invasive cancer. Usual ductal hyperplasia was defined as a proliferative lesion with cells that had relatively few cytoplasm with often overlapping (small) nuclei which were irregular in size and shape. Lumina, if present, were irregular in size, shape and distribution, and streaming of nuclei around the lumina often occurred [24].

2.2. Feulgen staining

Four μm sections were cut from paraffin-embedded tissue, deparaffinized, rehydrated, postfixed in Boehm-Sprenger fixative and stained with a modified Feulgen procedure as described before [5]. In short, slides were incubated for 60 minutes in 5 N HCl, followed by a thionin-SO₂ staining for 60 minutes, and finally rinsed in 0.5% sodium metabisulfite (aqueous solution, pH = 1.9). Slides were dehydrated and mounted with cytoseal 60 mounting medium (VWR Scientific).

2.3. Image cytometry

Image cytometry was performed at the Cancer Imaging Department of the British Columbia Cancer Agency in Vancouver, Canada. Measurements were

performed using the Cyto-Savant (Oncometrics Imaging Corp., Vancouver Canada) device, an automated digital imaging system which has been described previously [25]. The device was used to acquire autofocussed digital images of manually segmented cell nuclei on histologic sections, with spatial resolution resolution of 0.34 μm , and photometric resolution of 255 grey levels (S/N ratio \sim 150 : 1).

From each tissue section, nuclear images were acquired for 25–75 lymphocytes (internal diploid control), 50–300 nuclei from usual ductal hyperplastic lesion, and 50–200 cells from normal-appearing ducts and acini. The number of selected nuclei depended on how many cells of interest were present on the analyzed slide. Only non-overlapping nuclei that appeared to be in focus were selected. Segmentation of the selected nuclei was automatic. Manual correction of the nuclear contour was applied in the instances of touching, but not overlapping nuclei (which were discarded). Normal lymphocytes were used as internal control cells to normalize the features for the variations in staining intensity.

128 nuclear features were calculated for each nucleus. Morphometric feature measurements were according to calculations which have been published in detail elsewhere [9]. In brief, features can be divided into several categories. (1) Morphometrical features, describing the size and shape of nuclei, including nuclear area, shape factors, and features which characterize irregularities in the contours of the nucleus. (2) Photometric features, including the integrated optical density of the nucleus (proportional to the DNA content, normalized to 1.0 for diploid cells using lymphocytes as internal diploid controls), as well as statistics which describe the distribution of optical density (OD) within the nucleus (mean, skewness, kurtosis). (3) Discrete texture features, which rely on the distinction of three classes of chromatin condensation states, i.e., high, medium, and low density chromatin. Discrete texture features describe the relative amounts of DNA in each condensation state, as well as the number, size, and spatial distribution of discrete particles of chromatin in each of these states. (4) Markovian texture features, which are statistics describing the distribution of light intensity between adjacent pixels (e.g., contrast, correlation, energy), (5) fractal texture features, which describe the overall complexity and contrast of chromatin patterns, and (6) run length texture features, which describe the number and photometric distribution of grey level runs (consecutive pixels in the image with the same grey level value) (e.g., short runs, long runs).

2.4. Statistics

Population statistics were calculated for each nuclear feature over nuclei from individual slides, so that each patient record corresponded to a measurement of the mean and standard deviation of the 128 features. The distribution of these slide statistics between cases with and without invasive breast cancer were compared by non-parametric Mann–Whitney statistics. For this purpose, we used separately morphologically normal epithelial cells as well as hyperplastic cells. Secondly, as it is possible that variations in normal cells may be attributed to sectioning and tissue processing artifacts, and that these artifacts may obscure significant differences in hyperplastic cells, a method for normalization of the measurements on hyperplastic cells was explored. The slide means from measurements of hyperplastic cells were expressed in terms of their deviation from the corresponding measurements of normal cells. A standard normal form was obtained by dividing these deviations by the corresponding standard deviation of normal cells. Thus, a z -score is obtained for a feature measurement of hyperplastic cells according to the formula:

$$z\text{-score} = [\text{mean of feature (hyperplastic cells)} - \text{mean of feature (normal cells)}] / \text{SD of feature (normal cells)}.$$

Thirdly, discriminant function analysis was performed to distinguish between the groups of cases with and without synchronous invasive cancer. Since the size of the sample ($n = 71$) was relatively small, the use of multivariate classifiers was restricted to the use of pairs of uncorrelated feature measurements.

3. Results

Many nuclear features of normal-appearing cells and separately of usual ductal hyperplastic cells were significantly different between cases with and without synchronous invasive cancer. Figure 1 shows an example of an usual ductal hyperplasia with and without adjacent invasive carcinoma. In the normal-appearing cells as well as in the hyperplastic cells, differences in chromatin pattern are seen between the two cases. The most significant different features are summarized in Tables 1 to 3. The t -statistic is listed in each of the tables in order to show the direction and magnitude of the effect. A positive t -value indicates that the corre-

sponding value of the nuclear feature is decreased in the cells of cases with synchronous invasive cancer.

Table 1 lists the results of tests performed on measurements of cell images derived from normal-appearing ducts. Marginally significant differences in feature measurements between cases with and without adjacent invasive cancer are apparent, suggesting that MACs may be present in these nuclei. The positive values of the t -statistic indicate that the values of all significant nuclear features are decreased in lesions with invasive cancer. Considering the slide standard deviations, this is potentially important since it may indicate that MACs correspond to an effect that generates a more uniform population of cells. A morphological translation of the values listed for feature means, in terms of the cytological features of cells from normal ducts, suggests a redistribution of chromatin from low density regions to medium and high density chromatin in association with carcinoma. Additionally, the radial dispersion of medium and high density chromatin is seen to be decreased in normal cells from lesions with concurrent carcinoma. That is, there is an overall redistribution of these chromatin regions away from the periphery of the cell nucleus. A redistribution of chromatin is also seen with low density chromatin, which is observed to be distributed with greater symmetry in cells associated with carcinoma.

Table 2 lists the results of measurements on cells from usual ductal hyperplastic ducts, comparing cases with and without synchronous cancer. The t -statistics show a more heterogeneous pattern, indicating a significant increase in the overall contrast of chromatin patterns in hyperplastic cells from cases with cancer. In addition, lesions with synchronous cancer show an increase in the number of discrete particles of medium density chromatin, and an increase in the heterogeneity of cell populations with respect to this parameter. However, there is no significant redistribution of chromatin within high, medium, and low density regions in the hyperplastic cells in cases with invasion compared to those without. The number of short runs in these cell images is increased in association with carcinoma, indicating an increase in the complexity of chromatin patterns. High density chromatin is also seen to be more peripherally distributed in association with carcinoma.

The results for the z -score approach on the ductal hyperplastic cells are shown in Table 3. More features (in total 28) were now significant at the $p = 0.04$ level of which the most significant ones are listed in Table 3, suggesting that this approach is indeed use-

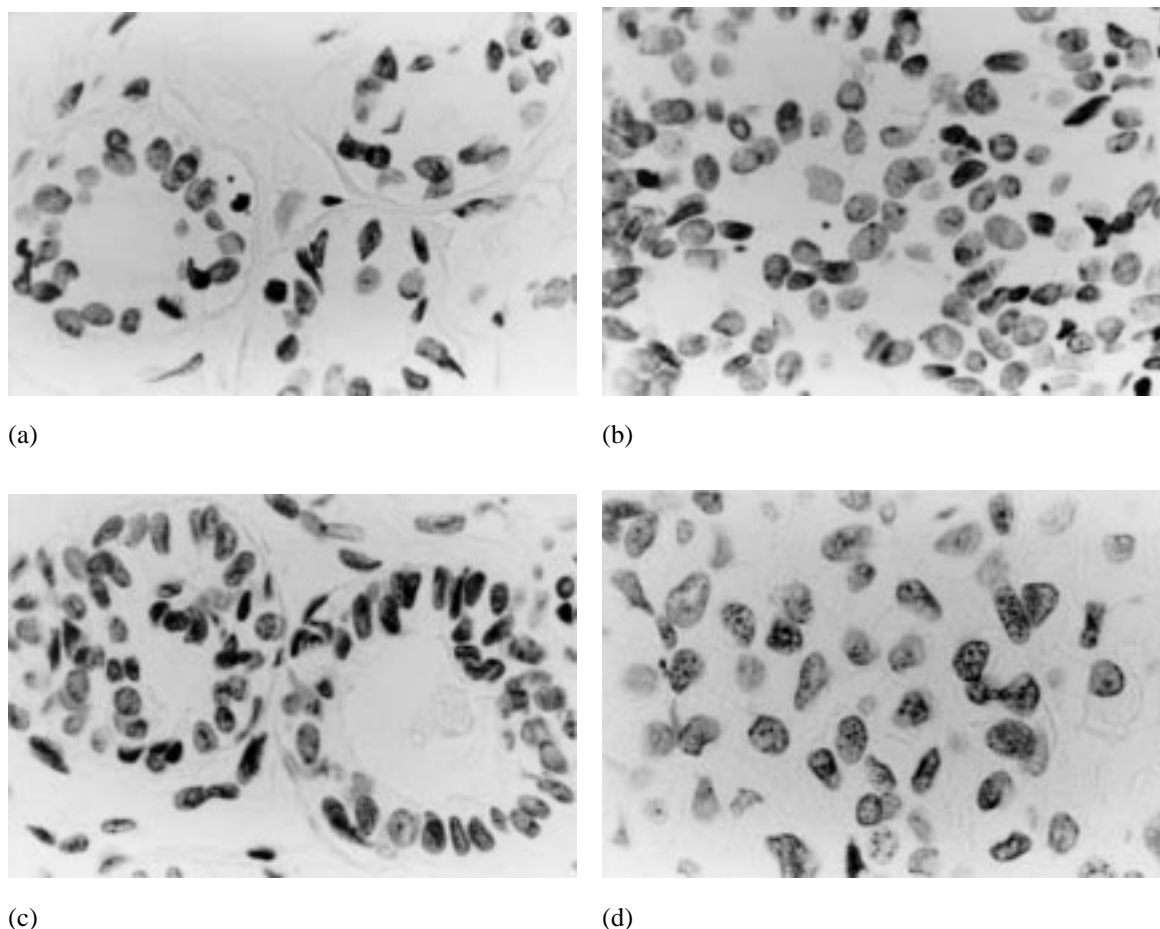


Fig. 1. Example of an usual ductal hyperplasia patient without adjacent invasive carcinoma (a, b) and an usual ductal hyperplasia patient with adjacent invasive carcinoma (c, d). Differences in chromatin patterns are seen between normal-appearing ducts (a and c), and even more apparent in the hyperplastic cells (b and d). Slides were Feulgen stained as described in Material and methods (100 \times objective magnification).

ful for coping with artefacts. Interpretation of the cytologic features are consistent with the analysis of results from Table 2, where the significant features from z -scores show the same direction of change in association with carcinoma. Most significantly the z -scores reveal a highly significant increase in the amount of high density chromatin in association with carcinoma, with a corresponding increase in the mean optical density of the nuclei. This also corresponds to a decrease in the mean optical intensity of nuclei, and to a reduced kurtosis of optical density in lesions associated with carcinoma. Again, medium density chromatin particles are seen to be more peripherally distributed over the nucleus. The number of short runs is increased in association with carcinoma, showing a more complex and highly textured chromatin pattern.

Discriminant function analysis to select pairs of slide nuclear features of normal or hyperplastic cells

which best separated the groups with and without invasion worked best in the ductal hyperplastic cells (Fig. 2). Best separation was found by using the parameters mean contrast and SD of fractal 1 area. In the figure it is apparent that the slide mean of the contrast parameter is distinctly increased in a substantial number of hyperplasias associated with carcinoma, and that there is a group of hyperplastic lesions with markedly increased variance for the fractal area parameter. Using these 2 parameters for hyperplastic nuclei, 80% classification accuracy could be reached to distinguish lesions with and without invasive cancer. However, many lesions fell quite close to the classification line with a low posteriori probability and extreme outliers were also found (such as the case with the lowest contrast and very low fractal area 1 value which had adjacent invasive cancer in Fig. 2). Similar analyses were performed for normal cells with an overall classification

Table 1

Significance values (Mann–Whitney test) for significant differences in feature measurements on normal cells from ductal hyperplasia cases with and without concurrent invasive carcinoma

| Feature | Slide mean or SD | <i>t</i> -statistic | <i>p</i> -value (MW) |
|--|------------------|---------------------|----------------------|
| Morphological feature: | | | |
| Irregularity in nuclear contour | Slide mean | 1.99 | 0.015 |
| Discrete texture features: | | | |
| Asymmetry of low density chromatin distribution | Slide SD | 2.16 | 0.013 |
| Ratio of DNA amount of low- vs medium density chromatin regions | Slide SD | 2.09 | 0.015 |
| Ratio of DNA amount of low- vs high density chromatin regions | Slide mean | 2.27 | 0.030 |
| Ratio of DNA amount of low- vs medium/high density chromatin regions | Slide mean | 1.96 | 0.036 |
| Radial dispersion of low density chromatin regions | Slide SD | 2.27 | 0.025 |
| Radial dispersion of medium density chromatin regions | Slide mean | 2.21 | 0.035 |
| Radial dispersion of medium density chromatin regions | Slide SD | 1.27 | 0.033 |
| Radial dispersion of medium + high density chromatin regions | Slide mean | 1.03 | 0.030 |
| Number of discrete particles of medium density chromatin | Slide mean | 2.16 | 0.036 |

For each feature, slide means and SD were calculated. Significance values greater than $p = 0.04$ are not listed.

Table 2

Significance values (Mann–Whitney test) for significant differences in feature measurements on hyperplastic cells from ductal hyperplasia cases with and without concurrent invasive carcinoma

| Feature | Slide mean or SD | <i>t</i> -statistic | <i>p</i> -value (MW) |
|--|------------------|---------------------|----------------------|
| Discrete texture features: | | | |
| Number of discrete particles of medium density chromatin | Slide mean | −2.72 | 0.014 |
| Number of discrete particles of medium density chromatin | Slide SD | −2.72 | 0.009 |
| Radial dispersion of high density chromatin regions | Slide mean | −1.60 | 0.037 |
| Markovian texture features: | | | |
| Contrast between adjacent pixels | Slide mean | −2.78 | 0.004 |
| Run length texture features: | | | |
| Number of short grey level runs (average of four directions) | Slide mean | −1.94 | 0.036 |
| Number of short grey level runs (average of four directions) | Slide SD | 2.31 | 0.017 |
| Number of short runs in direction which yields the maximum value | Slide mean | −1.88 | 0.037 |
| Number of short runs in direction which yields the maximum value | Slide SD | 2.43 | 0.004 |

For each feature, slide means and SD were calculated. Significance values greater than $p = 0.04$ are not listed.

Table 3

Significance values (Mann–Whitney test) for significant differences in feature measurements on hyperplastic cells from ductal hyperplasia cases with and without concurrent invasive carcinoma using the z -score approach

| Feature (z -score) | t -statistic | p -value (MW) |
|---|----------------|-----------------|
| Discrete texture features: | | |
| Radial dispersion of medium density chromatin regions | −2.71 | 0.009 |
| Relative area of nucleus occupied by high density chromatin | −2.63 | 0.007 |
| Relative amount of high density chromatin | −2.61 | 0.008 |
| Run length texture features: | | |
| Number of short grey level runs in direction which yields the maximum value | −2.99 | 0.007 |
| Photometric features: | | |
| Mean optical intensity of nucleus | 2.74 | 0.007 |
| Mean optical density of nucleus | −2.81 | 0.006 |
| Kurtosis of optical density distribution | 2.85 | 0.005 |

For each feature, slide means and SD were calculated. Significance values greater than $p = 0.01$ are not listed.

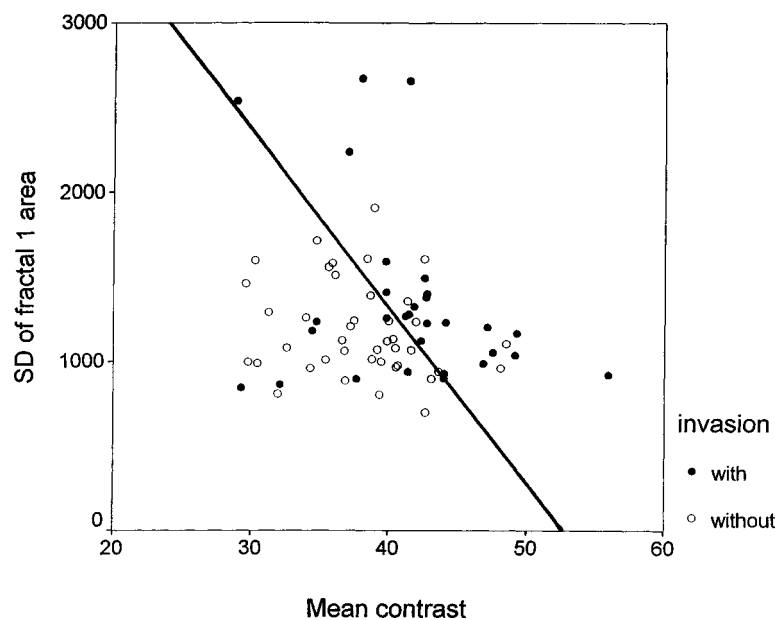


Fig. 2. Best separation of cases with (●) or without (○) invasive breast cancer, using image cytometry on ductal hyperplastic nuclei. Classification accuracy was 80% with discriminant function analysis.

accuracy of 67%, and using the z -score for hyperplastic cells with an accuracy of 68%.

4. Discussion

The presence of malignancy-associated changes (MACs) has been described in several tissues [2,4,10,

12,14,16,17,19,20,22,23,26,27]. However, the biological nature of MACs is not yet fully understood. It is not clear whether MACs develop in response to factors produced by the malignant tumor, such as chemokines and growth factors, or that it is an intrinsic first indication of the malignant potential of the tissue. The development of cancer is a multistep process, and it is possible that the development of MACs are the re-

sults of early changes in this process. The existence of MACs in a benign biopsy could therefore be suggestive of a higher risk of developing malignancy. However, it is difficult to determine the underlying cell biological changes which causes changes in chromatin patterns of normal-appearing cells. In any case, if MACs proceed the onset of cancer, it is possible that they may be modulated, and could be used as intermediate end point markers to monitor the effect of chemopreventive compounds, and perhaps for risk assessment of patients with premalignant lesions.

In the present study, we found significant differences between several nuclear features from normal ducts between patients with or without synchronous invasive breast cancer. This implies that also in breast tissue a MAC effect exists, which was also indicated by the results of Susnik et al. [27]. This supports the results of genetic studies which found loss of heterozygosity and microsatellite instability in morphologically normal lobules adjacent to breast cancers, suggesting that genetic alterations may already occur before light microscopic morphological abnormalities can be seen [7,18]. Also by measuring ductal hyperplastic cells, significant nuclear differences could be found between cases with and without synchronous cancer, especially when corrected for sectioning and tissue processing artifacts. Other studies also describe differences in preinvasive breast lesions adjacent to invasive carcinoma compared to lesions without adjacent invasion [1,28,29]. Quantitative nuclear features of ductal carcinoma *in situ* (DCIS) lesions could be used to predict the presence or absence of adjacent invasive breast carcinoma [28]. Overexpression of several proto-oncogenes, like p53 and HER-2/*neu*, was more frequently found in DCIS adjacent to invasive carcinoma than in pure lesions [1,29]. However, DCIS is considered to be a more advanced preinvasive breast lesion than usual ductal hyperplasia, and the described differences in proto-oncogene expression between cases with or without cancer were not found in usual ductal hyperplasia [21]. It would be ideal if a quite easy technique like image cytometry on normal or non-malignant cells could be used to predict the presence of invasive breast carcinoma (at distance) in an individual case. However, the use of discriminant analysis in the present study was restricted because of the relatively small group, and therefore analysis was based on only 2 features. To really test the reliability of our results, i.e., the presence of MACs in breast tissue determined with image cytometry, an independent training and test set of cases should be used [30].

In our study, the group was too small to divide into training and test set. We designed a classification rule using only 2 features because of the small sample size, but we were not able to estimate the performance of this rule on an independent data set. This means that our result of 80% classification accuracy may be over-optimistic, as illustrated by Schulerud et al. [30]. Therefore, we were very restrained in drawing conclusions from this multivariate analysis.

Another possible way to improve our data is to perform image cytometry on whole cell suspensions. The drawback of measuring nuclear features on tissue sections is the cutting of the nuclei and the slight variation in section thickness which may influence the measurements to some extent. While a number of methods for correcting for this artifact have been discussed in literature, none of these have been found to be satisfactory. It is recognized that it is always preferable, yet not always possible, to obtain intact, dispersed cells for cytometric measurements.

Besides the above mentioned problems with image cytometry on tissue sections, there are also statistical significance problems in analyzing image cytometry results in general. We evaluated 256 features (128 mean and 128 standard deviation features) which is many for the sample size of 71 cases in total. Due to chance, about 10 features would be significantly different between the two groups at the 4% level. This was also on average the number of significant differences we found in our study. A way to correct for multiple comparisons is to use the Bonferroni procedure, i.e., dividing the significance level by the number of features resulting in an adjusted significance level. However, in our and probably also other image cytometric studies, many features are correlated and thus simply adjusting the significance level would not be correct. A few of the differences we found were highly significant, especially for the measurements on the hyperplastic cells, implying that these were at least real differences. After correction for possible artefacts by using *z*-scores, even more features were highly significantly different between the two groups, supporting our believe in the presence of MACs in breast tissue. It can however not be ruled out that part of this improvement is due to the added degree of freedom which the combination of several measurements introduces.

Despite the above mentioned statistical problems, we believe that there is enough evidence that MACs exists in breast tissue. When our results can be confirmed by independent studies, than image cytometry on normal or early preinvasive breast lesions could be

clinically meaningful in several ways. First, presence of MACs in normal breast cells may provide evidence for a cancer somewhere in the breast. Second, MACs may be used to monitor the effect of chemopreventive agents, especially in patients with a hereditary predisposition. Third, MACs may prove to be useful for risk assessment of patients with preinvasive breast lesions. These potential applications of MAC assessment by image cytometry of the breast deserve to be further studied.

In conclusion, image cytometry on breast tissue sections shows that malignancy-associated changes can be found in normal as well as in usual ductal hyperplastic breast cells. This could be clinically relevant for prediction of presence of synchronous breast cancer, patients with occult breast cancer, and to monitor the effect of chemopreventive agents.

Acknowledgements

We would like to thank Paul Lam for his expert support. This project was supported by the Dutch Cancer Society grant no. 95-930.

References

- [1] D.C. Allred, G.M. Clark, R. Molina, A.K. Tandon, S.J. Schnitt, K.W. Gilchrist, C.K. Osborne, D.C. Tormey and W.L. McGuire, Overexpression of HER-2/neu and its relationship with other prognostic factors change during the progression of in situ to invasive breast cancer, *Hum. Pathol.* **23** (1992), 974–979.
- [2] G. Anderson, C. MacAulay, J. Maticic, D. Garner and B. Palcic, The use of an automated image cytometer for screening and quantitative assessment of cervical lesions in the British Columbia Cervical Smear Screening Programme, *Cytopathology* **8** (1997), 298–312.
- [3] J.P.A. Baak and P.C. Diegenbach, Quantitative nuclear image analysis: differentiation between normal, hyperplastic, and malignant appearing uterine glands in a paraffin section. I. Elementary features for differentiation, *Eur. J. Obstet. Gynecol. Reprod. Biol.* **7** (1977), 33–42.
- [4] M. Bibbo, A.G. Montag, E. Lerma-Puertas, H.E. Dytch, S. Leelakusolvong and P.H. Bartels, Karyometric marker features in tissue adjacent to invasive cervical carcinomas, *Anal. Quant. Cytol. Histol.* **11** (1989), 281–285.
- [5] H.K. Choi, J. Vasko, E. Bengtsson, T. Jakrans, P.U. Malmstroem, K. Wester and C. Busch, Grading of transitional cell bladder carcinoma by texture analysis of histological sections, *Anal. Cell. Pathol.* **6** (1994), 327–343.
- [6] L. Deligdisch, C. Miranda, J. Barba and J. Gil, Ovarian dysplasia: nuclear texture analysis, *Cancer* **72** (1993), 3253–3257.
- [7] G. Deng, Y. Lu, G. Zlotnikov, A.D. Thor and H.S. Smith, Loss of heterozygosity in normal tissue adjacent to breast carcinomas, *Science* **274** (1996), 2057–2059.
- [8] P.C. Diegenbach and J.P.A. Baak, Quantitative nuclear image analysis: differentiation between normal, hyperplastic, and malignant appearing uterine glands in a paraffin section. IV. The use of Markov chain texture features in discriminant analysis, *Eur. J. Obstet. Gynecol. Reprod. Biol.* **8** (1978), 157–162.
- [9] A. Doudkine, C. MacAulay, N. Poulin and B. Palcic, Nuclear texture measurements in image cytometry, *Pathologica* **87** (1995), 286–299.
- [10] R.R. Finch, A classification of nuclear aberrations in relation to malignancy-associated changes, *Acta Cytol.* **15** (1971), 553–558.
- [11] C. Francois, C. Decaestecker, O. DeLathouwer, C. Moreno, A. Peltier, T. Roumeguere, A. Danguy, J.L. Pasteels, E. Wespes, I. Salmon, R. van Velthoven and R. Kiss, Improving the prognostic value of histopathological grading and clinical staging in renal cell carcinomas by means of computer-assisted microscopy, *J. Pathol.* **187** (1999), 13–20.
- [12] M. Guillaud, A. Doudkine, D. Garner, C. MacAulay and B. Palcic, Malignancy associated changes in cervical smears: systematic changes in cytometric features with the grade of dysplasia, *Anal. Cell. Pathol.* **9** (1995), 191–204.
- [13] A.G. Hanselaar, N. Poulin, M.M. Pahlplatz, D. Garner, C. MacAulay, J. Maticic, J. LeRiche and B. Palcic, DNA-cytometry of progressive and regressive cervical intraepithelial neoplasia, *Anal. Cell. Pathol.* **16** (1998), 11–27.
- [14] G. Haroske, S. Bergander, R. Konig and W. Meyer, Application of malignancy-associated changes of the cervical epithelium in a hierarchic classification concept, *Anal. Cell. Pathol.* **2** (1990), 189–198.
- [15] T. Jorgensen, K. Yogesan, K.J. Tveter, F. Skjorten and H.E. Danielsen, Nuclear texture analysis: a new prognostic tool in metastatic prostate cancer, *Cytometry* **24** (1996), 277–283.
- [16] H.U. Kasper, G. Haroske, U. Geissler, W. Meyer and K.D. Kunze, Diagnostic and prognostic relevance of malignancy-associated changes in cervical smears, *Anal. Quant. Cytol. Histol.* **19** (1997), 482–488.
- [17] H.J. Kwikkel, T. Timmers, M.E. Boon, M.M. van Rijswijk and J.G. Stolk, Relation of quantitative features of visually normal intermediate cells in cervical intraepithelial neoplasia I and II smears to progression or nonprogression of the lesion, *Anal. Quant. Cytol. Histol.* **9** (1987), 405–410.
- [18] P.S. Larson, A. DelasMorenas, L.A. Cupples, K. Huang and C.L. Rosenberg, Genetically abnormal clones in histologically normal breast tissue, *Am. J. Pathol.* **152** (1998), 1591–1598.
- [19] C. MacAulay, S. Lam, P.W. Payne, J.C. LeRiche and B. Palcic, Malignancy-associated changes in bronchial epithelial cells in biopsy specimens, *Anal. Quant. Cytol. Histol.* **17** (1995), 55–61.
- [20] T. Mairinger, G. Mikuz and A. Gschwendtner, Nuclear chromatin texture analysis of nonmalignant tissue can detect adjacent prostatic adenocarcinoma, *Prostate* **41** (1999), 12–19.
- [21] E.C.M. Mommers, P.J. van Diest, A.M. Leonhart, C.J.L.M. Meijer and J.P.A. Baak, Expression of proliferation and apoptosis-related proteins in usual ductal hyperplasia of the breast, *Hum. Pathol.* **29** (1998), 1539–1545.

- [22] A.G. Montag, P.H. Bartels, E. Lerma-Puertas, H.E. Dytch, S. Leelakusolvong and M. Bibbo, Karyometric marker features in tissue adjacent to in situ cervical carcinomas, *Anal. Quant. Cytol. Histol.* **11** (1989), 275–280.
- [23] H.E. Nieburgs, A.F. Goldberg, B. Bertini, J. Silagi, B. Pacheco and H. Reisman, Malignancy-associated changes in blood and bone marrow cells of patients with malignant tumors, *Acta Cytol.* **11** (1967), 415–423.
- [24] D.L. Page, T.J. Anderson and L.W. Rogers, Epithelial hyperplasia, and Carcinoma in situ, in: *Diagnostic Histopathology of the Breast*, D.L. Page and T.J. Anderson, eds, Churchill Livingstone, Edinburgh, 1987, pp. 120–192.
- [25] B. Palcic, B. Susnik, D. Garner and I. Olivotto, Quantitative evaluation of malignant potential of early breast cancer using high resolution image cytometry, *J. Cell. Biochem.* **17G** (1993), 107–113.
- [26] B. Palcic, D.M. Garner and C.E. MacAulay, Image cytometry and chemoprevention in cervical cancer, *J. Cell. Biochem. Suppl.* **23** (1995), 43–54.
- [27] B. Susnik, A. Worth, J. LeRiche and B. Palcic, Malignancy-associated changes in the breast: changes in chromatin distribution in epithelial cells in normal-appearing tissue adjacent to carcinoma, *Anal. Quant. Cytol. Histol.* **17** (1995), 62–68.
- [28] B. Susnik, A. Worth, B. Palcic, N. Poulin and J. LeRiche, Differences in quantitative nuclear features between ductal carcinoma in situ with and without accompanying invasive carcinoma in the surrounding breast, *Anal. Cell. Pathol.* **8** (1995), 39–52.
- [29] Y. Umekita, T. Takasaki and H. Yoshida, Expression of p53 protein in benign epithelial hyperplasia, atypical ductal hyperplasia, non-invasive and invasive mammary carcinoma: an immunohistochemical study, *Virchows Arch.* **24** (1994), 491–494.
- [30] H. Schulerud, G.B. Kristenen, K. Liestol, L. Vlatkovic, A. Reith, F. Albrechtsen and H.E. Danielsen, A review of caveats in statistical nuclear image analysis, *Anal. Cell. Pathol.* **16** (1998), 63–82.